

The Distribution of Ammonia and Its Photochemical Products on Jupiter

S. K. ATREYA,¹ T. M. DONAHUE,¹ AND W. R. KUHN^{1,2}

*Department of Atmospheric and Oceanic Science, Space Physics Research Laboratory,
The University of Michigan, Ann Arbor, Michigan 48109*

Received June 15, 1976; revised January 3, 1977

Altitude profiles of ammonia and its photochemical products are generated in the light of the new measurements of the Jovian temperature structure, eddy transport coefficient, improved chemical scheme, and rate constants. Realistic limits are placed on the concentration of hydrazine which may participate in the recycling of ammonia on Jupiter. The maximum hydrazine ice production rate is calculated to be about $1.3 \text{ mg m}^{-2}/\text{Jovian day}$. The distribution of nitrogen gas is presented with and without supersaturation of hydrazine. The nitrogen mixing ratio near the ammonia cloud top is estimated to be in the range of 10^{-9} to 10^{-11} . An appreciable latitudinal variation in the ammonia concentration is expected.

INTRODUCTION

Several new laboratory and *in situ* measurements pertinent to the problem of ammonia on Jupiter have become available since Strobel (1973) published his calculations of the NH_3 photochemistry. The Jovian temperature profile down to the ammonia cloud top has been inferred with a degree of accuracy adequate for the prediction of some interesting atmospheric properties from the data collected by both the infrared radiometer and the radio occultation techniques used on Pioneers 10 and 11. New insight into the possible range of values for the eddy mixing coefficient is provided by the Jovian Lyman α airglow measurements. Additional chemical reactions and improved laboratory measurements of rate constants of some pertinent reactions are now available. In view of this new knowledge and the possible

Jupiter Orbiter Probe Mission whose atmospheric sampling instruments would be designed to measure the various gaseous species in the lower atmosphere of Jupiter, we have carried out calculations which yield new estimates of the distribution of ammonia and its photochemical products. Sensitivity studies have also been made for several possible variations of the eddy transport coefficient. In addition, the question of hydrazine (N_2H_4) condensation is discussed and extreme profiles of "gaseous" hydrazine as a function of Jovian altitude are generated along with the corresponding distribution of nitrogen gas. Some insight into the diurnal and latitudinal behavior of the gases is provided and important new or improved laboratory measurements are identified.

MODELS

For the present calculations we assume the temperature profile as inferred from the Pioneers 10 and 11 data (Hunten, 1976). The temperature varies from 165°K

¹The authors have contributed equally to this study.

²Also at Chemical Evolution Branch, NASA-Ames Research Center, California 94035.

TABLE I
RELEVANT CHEMICAL REACTIONS AND ASSOCIATED RATE CONSTANTS

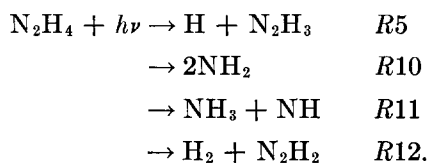
Reaction number	Reaction	Rate constant ^a	Reference
R1	$\text{NH}_3 + h\nu \rightarrow \text{NH}_2(X) + \text{H}$	$J(\text{NH}_3)$	See text
R2	$\text{NH}_2(X) + \text{H} \xrightarrow{+M} \text{NH}_3$	$k_2 = 6 \times 10^{-20}[M]/(1 + 3 \times 10^{-20}[M])$	Gorden <i>et al.</i> (1971)
R3	$\text{NH}_2(X) + \text{NH}_2(X) \xrightarrow{+M} \text{N}_2\text{H}_4$	$k_3 = 1 \times 10^{-10}$	Gorden <i>et al.</i> (1971)
R4	$\text{N}_2\text{H}_4 + \text{H} \rightarrow \text{N}_2\text{H}_3 + \text{H}_2$	$k_4 = 9.87 \times 10^{-12} \exp(-1198/T)$	Stief and Payne (1976)
R5	$\text{N}_2\text{H}_4 + h\nu \rightarrow \text{N}_2\text{H}_3 + \text{H}$	$J(\text{N}_2\text{H}_4)$	See text
R6	$\text{N}_2\text{H}_3 + \text{H} \rightarrow 2\text{NH}_2$	$k_6 = 2.7 \times 10^{-12}$	Gehring <i>et al.</i> (1969)
R7	$\text{H} + \text{H} + M \rightarrow \text{H}_2 + M$	$k_7 = 8 \times 10^{-32}(300/T)^{0.6}$	Ham <i>et al.</i> (1970)
R8	$\text{N}_2\text{H}_3 + \text{N}_2\text{H}_3 \rightarrow 2\text{NH}_3 + \text{N}_2$	$k_8 \ll k_9$	Stief (1976, personal communication)
R9	$\text{N}_2\text{H}_3 + \text{N}_2\text{H}_3 \rightarrow \text{N}_2\text{H}_4 + \text{N}_2\text{H}_2$ $\rightarrow \text{N}_2\text{H}_4 + \text{N}_2 + \text{H}_2$	$k_9 = 6 \times 10^{-11}$	Stief (1976, personal communication)

^a Rate constants (k 's) are given in $\text{cm}^3 \text{sec}^{-1}$ for two-body reactions and in $\text{cm}^6 \text{sec}^{-1}$ for three-body reactions. Photodissociation rates $J(\text{NH}_3)$ and $J(\text{N}_2\text{H}_4)$ are given in sec^{-1} .

at 1000 mbar to 148°K at 10 mbar with a distinct temperature inversion (110°K) around the 100-mbar pressure level. The Pioneer 10 Lyman α airglow measurements (Carlson and Judge, 1974) seem to indicate an eddy diffusion coefficient of the order of $3 \times 10^{8 \pm 1} \text{cm}^2 \text{sec}^{-1}$ with a highly uncertain homopause. However, the recent OAO-Copernicus measurements (Barker, 1976) give a Lyman α intensity which may be up to four times greater than that interpreted by Carlson and Judge from their photometer data. Thus the Copernicus data imply a smaller value of eddy diffusion coefficient K . We have made calculations with $K \propto 1/M$ and $K \propto 1/M^{1/2}$ (see, e.g., Lindzen, 1971), both with an assumed tropopause value of $K_0 = 2 \times 10^4 \text{cm}^2 \text{sec}^{-1}$ after Tomasko (1974). Sensitivity studies are also done with $K_0 = 2 \times 10^3$ and $2 \times 10^5 \text{cm}^2 \text{sec}^{-1}$. We also consider the case with constant K of $2 \times 10^4 \text{cm}^2 \text{sec}^{-1}$, the value assumed by Strobel (1973). The $K \propto 1/M^{1/2}$ variation appears the most realistic; a $1/M$ variation produces an unacceptably high value of the eddy diffusion coefficient at the homopause.

The relevant chemical reactions and the associated rate constants are listed in Table I. Photolysis of ammonia longward of 1600 Å results in the formation of the

amidogen radical $\text{NH}_2(X)$ in the ground state. Reaction of $\text{NH}_2(X)$ with hydrogen recycles part of the ammonia while reaction with itself leads to the formation of hydrazine. Photolysis of gaseous N_2H_4 then gives the N_2H_3 radical which reacts with H to form NH_2 by the extraction reaction R6. N_2H_3 reacts with itself to produce N_2H_4 and N_2 (R9); the rate constant for R8 is much smaller than that for R9 (Stief, 1976, personal communication). The chemical reactions leading to the production of N_2 in this paper differ from Strobel's (1973) in that he considers production of N_2 directly from the photolysis of N_2H_4 and from the extraction reaction: $\text{N}_2\text{H}_3 + \text{H} \rightarrow \text{N}_2 + 2\text{H}_2$. Photolysis products of N_2H_4 by absorption of solar radiation longward of 1600 Å may be as follows:



Only the first one of these processes, R5, is dominant, while the rest have extremely low quantum yield (see Schurath and Schindler, 1970; Stief and Payne, 1976).

The rate constants k_2 , k_3 , and k_7 listed in Table I are the same as those used by

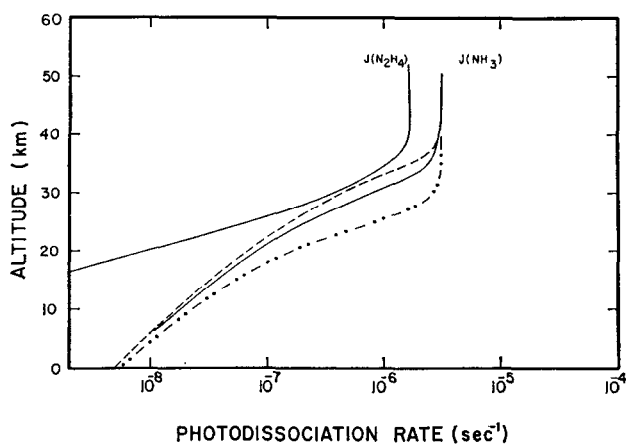


FIG. 1. Variation of ammonia and hydrazine photodissociation rates, $J(\text{NH}_3)$ and $J(\text{N}_2\text{H}_4)$, with height for several different atmospheric models. The reference altitude $z = 0$ km is taken at the 1-atm-pressure level. All model atmospheres have temperature varying with altitude in accordance with Hunten (1976). The rate constant k_4 is taken from the measurements of Stief and Payne (1976). The curve with $K = 2 \times 10^4 \text{ cm}^2 \text{ sec}^{-1}$ refers to the model in which the eddy diffusion coefficient is constant over the entire altitude range. The other two curves correspond to K varying inversely and inversely as the square root of the atmospheric number density, M , with reference value of $K = K_0 = 2 \times 10^4 \text{ cm}^2 \text{ sec}^{-1}$ at the 1-atm-pressure level ($M = 2.9 \times 10^{19} \text{ cm}^{-3}$). — · — ·, $T(z)$, $K = 2 \times 10^4 \text{ cm}^2 \text{ sec}^{-1}$ (constant); —, $T(z)$, $K \propto 1/M^{1/2}$; ---, $T(z)$, $K \propto 1/M$.

Strobel (1973). Stief and Payne (1976) indicate that in the relevant temperature range k_4 may be up to a factor of 35 lower than the Francis and Jones (1971) value used in earlier calculations.

Photoabsorption by ammonia was calculated for wavelengths between 1600 and 2300 Å; at shorter wavelengths solar radiation is absorbed by methane whose abundance above the ammonia cloud top is substantially greater than that of ammonia. Solar fluxes are from Ackerman (1971) and photoabsorption cross sections of NH_3 and N_2H_4 are from Watanabe (1954), Thompson *et al.* (1963), and Schürgers and Welge (1968). Solar flux and cross sections were averaged over a 10-Å interval; because of the structure in the ammonia cross sections, the averaging interval is important. As discussed later, the major uncertainty in the calculations results from the choice of the eddy diffusion coefficient. Therefore we have not included secondary effects such as depletion of solar flux by

Rayleigh scattering (Strobel, 1973) and aerosols. For the "global average" model the solar flux was decreased by a factor of 0.5 and the mass path was doubled. A calculation for a latitude of 75° was also carried out; the effective zenith angle ξ (determined by averaging $\cos \xi$ over the daylight hours) is 80.5° which yields a solar attenuation of 0.165

One-dimensional steady-state coupled continuity and eddy transport equations were solved by a generalized Newton-Raphson's method (see, e.g., Ames, 1969). The step size was 1 km and the convergence criterion was 5%. With the exception of N_2 , the system was treated as a two-point boundary value problem. Large variations in the boundary values caused changes in the solutions within only a few kilometers of the boundaries located at 0 km (number density of $2.9 \times 10^{19} \text{ cm}^{-3}$) and 40 km. A flux lower boundary condition was assumed for nitrogen so that the downward flux was approximately equal to half

the upward flux of ammonia; thus our solutions represent a lower limit to N_2 concentrations.

RESULTS AND DISCUSSION

Photodissociation rates of ammonia and hydrazine, $J(NH_3)$ and $J(N_2H_4)$, are shown in Fig. 1 for the various assumptions on the model atmosphere. We show only one profile for N_2H_4 corresponding to the atmospheric model in which $K \propto 1/M^{1/2}$ (standard case). This calculation was based on the assumption that all the N_2H_4 generated in reaction R3 of Table I is in the gaseous state. As we shall see later, if hydrazine condenses at its saturation vapor pressure then the dissociation rate will simply be the value corresponding to an optical depth of zero. The photodissociation rates of NH_3 can be as much as a factor of 4 greater than Strobel's (1973) values. This difference is attributed to revised solar flux data which in some spectral

regions are twice as large as those used by Strobel. Also our spectral interval of 10 Å allows a realistic reproduction of the absorption cross sections of NH_3 .

The height distributions of ammonia and its photolysis products in terms of volume mixing ratios are shown in Fig. 2. The curves refer to an eddy diffusion coefficient $K \propto 1/M^{1/2}$. The solid line curves for N_2H_4 , N_2H_3 , and N_2 were calculated on the assumption that all the N_2H_4 resulting from the reaction R3 is in the gaseous phase. One would not expect this to be the case; e.g., at 20 km where the temperature is 130°K, the saturation number density is estimated to be about 10^5 cm^{-3} while the calculated density is 10^{10} cm^{-3} . Such a degree of supersaturation is most unlikely.

Our calculations also show in Fig. 2 the N_2H_4 , N_2H_3 , and N_2 distribution if hydrazine ice forms at the saturation vapor pressure. We have calculated the sublimation vapor pressure from data of Audreith

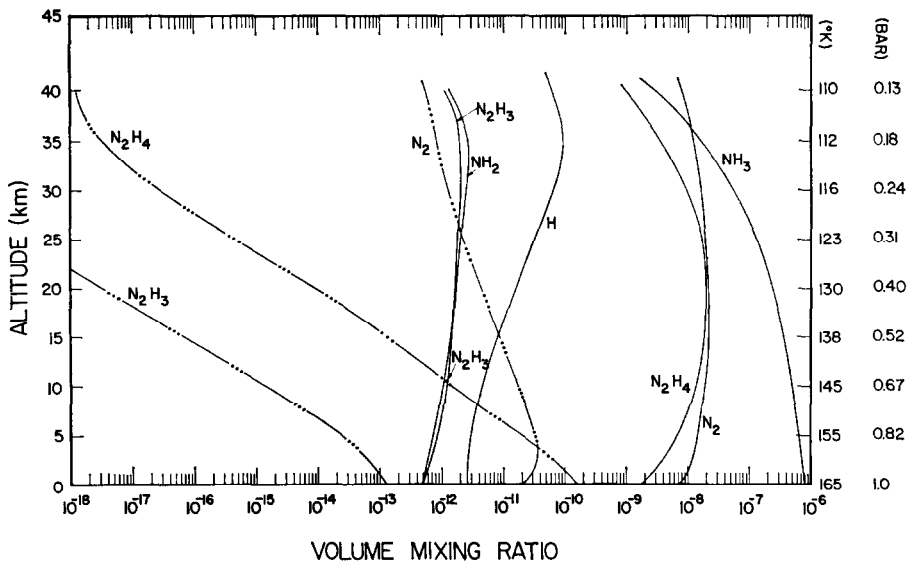


FIG. 2. Altitude profiles of volume mixing ratios of ammonia and its photochemical products for Hunten (1976) temperature profile and the $K \propto 1/M^{1/2}$ atmospheric model (solid line curves). The temperatures and pressures given on the right ordinate correspond to the altitudes shown on the left. The rate constant k_4 is that of Stief and Payne (1976). Curves illustrated by — · · — for N_2H_4 and N_2H_3 assume a saturation vapor mixing ratio. The resultant N_2 mixing ratio profile is shown by the — · · — curve.

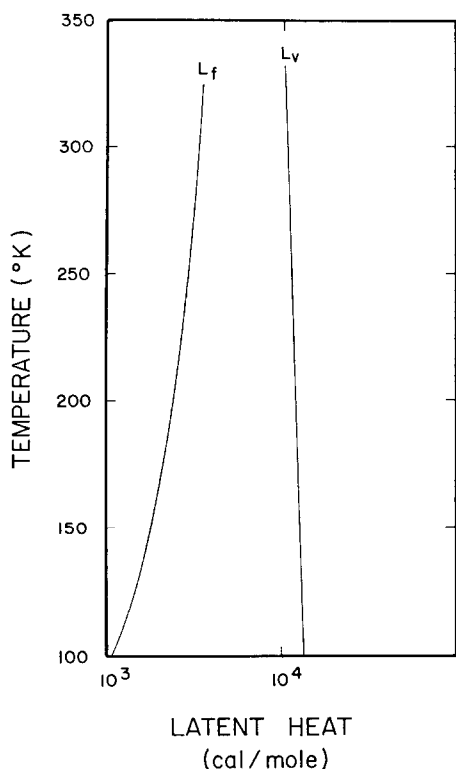


FIG. 3. Saturation vapor density (particles cm^{-3}) of N_2H_4 as a function of temperature from considerations of the latent heat of sublimation. The value of saturation vapor density of N_2H_4 at 100°K is 5.6 particles cm^{-3} .

and Ogg (1951) who give empirical expressions for the latent heats of vaporiza-

tion l_v and fusion l_f . It was necessary to extrapolate from these expressions to low temperatures since the relation for l_v is given for the range from 275 to 1000°K , while for l_f the range is 170 to 340°K . The temperature variation of the latent heats is not large (see Fig. 3) and we have estimated the latent heat of sublimation $l_s \sim l_v + l_f$ to be 1.4×10^4 cal/mole. The only measurement of which we are aware of the N_2H_4 vapor pressure over N_2H_4 ice is that of Scott *et al.* (1949), who find a pressure of 2.6 mm Hg at 273°K . From these data and the Clausius-Clapeyron equation, we find for the hydrazine saturation number density,

$$[\text{N}_2\text{H}_4]_s = (2.48 \times 10^{19}/T) \times \exp[25.8(1 - 273/T)]. \quad (1)$$

Note that over the temperature range of interest (~ 110 to 165°K) the saturation vapor density varies by about nine orders of magnitude (see Fig. 4). We have not used the Antoine equation (Scott *et al.*, 1949) to estimate the saturation vapor pressure of N_2H_4 since the expression was developed for the liquid-vapor phases. If this equation is extrapolated to the lower temperatures applicable to Jupiter, the difference between (1) and Antoine's equation varies up to a factor of 100.

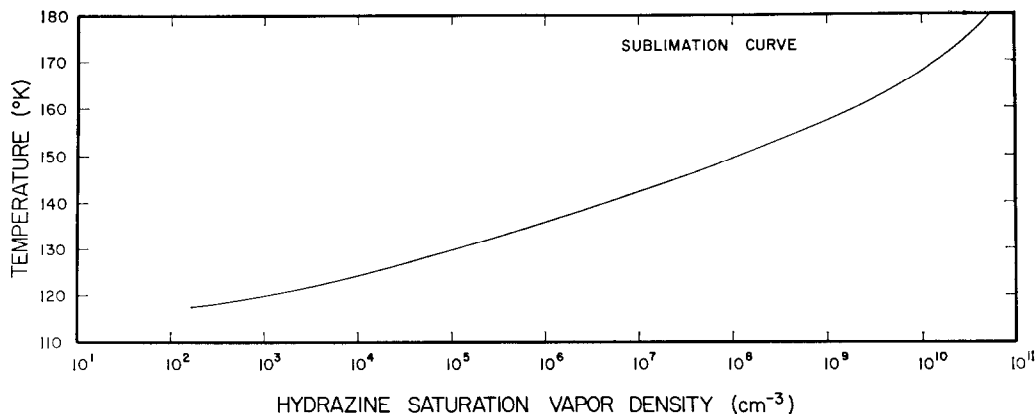


FIG. 4. Variation of the hydrazine latent heat of fusion l_f and latent heat of vaporization l_v with temperature.

The N_2H_4 concentrations which allow no supersaturation in Fig. 2 correspond to the saturation mixing ratio at the local temperature; i.e., the saturation value was less than the N_2H_4 calculated in the photochemical scheme which includes no condensation. If the atmosphere can sustain no more N_2H_4 in the gaseous phase than given by the saturation curve, the rest must be available for condensation. These two profiles which differ by many orders of magnitude over the altitude range represent the extremes for gaseous N_2H_4 . The trend toward a positive gradient around 40 km is due to the temperature inversion near this altitude.

The nitrogen concentration corresponding to the hydrazine saturation density is about a factor of 3×10^2 smaller near the cloud layer than the nitrogen calculated without any hydrazine condensation; at 40 km, however, the difference is about four orders of magnitude. The resultant N_2H_3 is several orders of magnitude less than hydrazine.

Mixing ratio profiles of NH_3 are shown for several variations of eddy coefficient in Fig. 5. For comparison we also show, by dotted line, Strobel's (1973) results calculated on the basis of a constant temperature of 120°K, a constant eddy diffusion coefficient $K = 2 \times 10^4 \text{ cm}^2 \text{ sec}^{-1}$, and a rate constant k_4 as given by Francis and Jones (1971). Although Strobel's (1973) results appear similar to the model with $K \propto 1/M^{1/2}$ in the present study, this is somewhat fortuitous. For example, using Strobel's reaction scheme and his model atmosphere, but with revised solar flux data and cross sections, we find NH_3 concentrations near 40 km to be some two orders of magnitude smaller than in the previous study. The present calculations apply to a mid-latitude case except for the long dashed curve which is for high latitude. One finds a wide variation in the NH_3 mixing ratio near the top with the choice of atmospheric parameters.

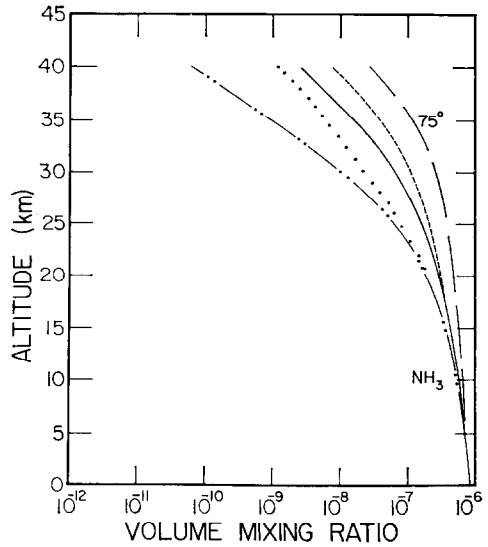


FIG. 5. Variation of ammonia mixing ratio with height for the various atmospheric models. The height scale is the same as in Fig. 1. — · —, $T(z)$, $K = 2 \times 10^4 \text{ cm}^2 \text{ sec}^{-1}$ (constant); —, $T(z)$, $K \propto 1/M^{1/2}$; ---, $T(z)$, $K \propto 1/M$; — · —, $T(z)$, $K \propto 1/M^{1/2}$, latitude = 75°; · · · ·, Strobel (1973).

As we have discussed earlier, perhaps the representative NH_3 distribution in the atmosphere of Jupiter is the one with $K \propto 1/M^{1/2}$, although the variation of NH_3 in this model and the one in which $K \propto 1/M$ is rather small.

There may be an appreciable variation in the ammonia concentration with latitude. At 75°, for example, the column abundance above 20 km is $5.3 \times 10^{18} \text{ cm}^{-2}$ while the mean global model yields about $2.7 \times 10^{18} \text{ cm}^{-2}$. At the equator the column abundance would be lower; latitudinal variations in NH_3 concentration between equator and pole above 30 km may be larger than two orders of magnitude if meridional transport is negligible. There may be significant variations in NH_3 from the mean global model due to the varying solar zenith angle as well as diurnal variations in the photolysis products. At nighttime, there is little variation in NH_3 , but NH_2 (see Fig. 6) decays rapidly to N_2H_4 .

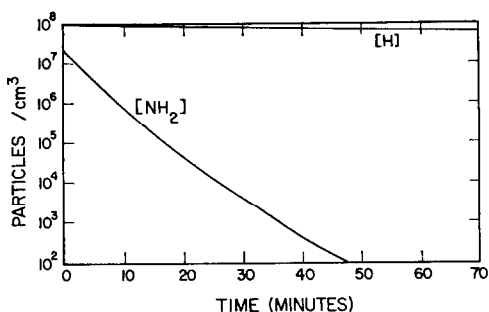


FIG. 6. Variation of NH_2 and H at night in the Jovian atmosphere. The height is approximately 20 km.

with a relaxation time of about 5 min. These calculations assumed the steady-state model as the initial condition and the photochemical equations were solved by the Runge-Kutta method. A study of the full time-dependent problem is in progress and will be reported subsequently.

CONCLUDING REMARKS

Jovian ammonia chemistry has been reevaluated in the light of improved solar flux data, chemical reactions, reaction rates, eddy diffusion coefficients, and temperature structure. The hydrazine column density above the ammonia cloud top can vary from 1×10^{15} to $6 \times 10^{17} \text{ cm}^{-2}$ depending upon the degree of supersaturation. If saturation does not occur then virtually all the hydrazine produced would condense with the total N_2H_4 ice production rate of $6.9 \times 10^{10} \text{ molecules cm}^{-2} \text{ sec}^{-1}$ which corresponds to an amount of about 1.3 mg m^{-2} per Jovian day.

Nitrogen is the principal gaseous component of ammonia photochemistry. Its column abundance would vary with the degree of hydrazine saturation. Typical N_2 column densities should be about $3 \times 10^{-5} \text{ cm amagat}$ if there is no supersaturation of hydrazine, while if all the hydrazine remains in the gaseous state the column abundance would be about $3.4 \times 10^{-2} \text{ cm amagat}$. These calculations assumed an eddy diffusion coefficient at the ammonia

cloud top of $2 \times 10^4 \text{ cm}^2 \text{ sec}^{-1}$; however, an eddy diffusion coefficient of $2 \times 10^3 \text{ cm}^2 \text{ sec}^{-1}$ produces an N_2 concentration two orders of magnitude larger. If the value of K_0 were as small as $2 \times 10^2 \text{ cm}^2 \text{ sec}^{-1}$ as suggested by Sagan and Salpeter (1976), the N_2 mixing ratio would be on the order of 10^{-7} . The N_2 concentration we estimate near the ammonia cloud top may be within the realm of *in situ* detection with the present mass spectrometers, particularly those utilizing enrichment techniques.

The mean global ammonia profiles which we calculate are similar to the earlier study by Strobel (1973), i.e., the ammonia destruction rates are within a factor of 2. However, there may be significant latitudinal variations. In high latitudes, the column abundance because of a larger effective zenith angle is most likely several times that at the equator. The results presented here are strongly dependent on the eddy diffusion coefficient. For example, a decrease in the value of the eddy diffusion coefficient from 2×10^4 to $2 \times 10^3 \text{ cm}^2 \text{ sec}^{-1}$ at the ammonia cloud top results in about a sevenfold decrease in the column abundance of ammonia.

The range of distributions of N_2H_4 , N_2H_3 , and N_2 gases presented in this paper relies on the vapor pressure of N_2H_4 which we approximated from the Clausius-Clapeyron equation. A precise measurement of the hydrazine vapor pressure at the low temperatures (110–165°K) prevalent in the lower atmosphere of Jupiter is highly desirable.

ACKNOWLEDGMENTS

We have benefited from discussion with G. R. Carignan, S. Chang, B. C. Kennedy, L. J. Stief, D. F. Strobel, and S. Walters. This research was supported in part by NASA under Grants AURA-86303 (NASA/JPL Contract 7-100), NAS2-8992, and A17362B.

REFERENCES

ACKERMAN, M. (1971). Ultraviolet solar radiation related to mesospheric processes. In *Mesospheric*

- Models and Related Experiments* (G. Fiocco, Ed.), p. 149. Reidel, Dordrecht.
- AMES, W. F. (1969). *Numerical Methods for Partial Differential Equations*. Barnes and Noble, New York.
- AUDREITH, L. F., AND OGG, R. A. (1951). *The Chemistry of Hydrazine*. Wiley, New York.
- BARKER, E. S. (1976). Personal communication and paper presented at the Division of Planetary Science, 7th Annual Meeting, Austin, Texas, 31 March, 1976.
- CARLSON, R. W., AND JUDGE, D. L. (1974). Pioneer 10 ultraviolet photometer observations at Jupiter encounter. *J. Geophys. Res.* **79**, 3623.
- EBERSTEIN, I. J., AND GLASSMAN I. (1965). The gas phase decomposition of hydrazine and its methyl derivative. In *Proc. Xth Symposium (International) on Combustion*, p. 365. The Combustion Institute, Princeton, N. J.
- FRANCIS, P. D., AND JONES A. R. (1971). ESR measurement reaction between H atoms and N₂H₄. *J. Chem. Phys.* **54**, 5085.
- GEHRING, M., HOYERMAN, G., WAGNER, H. G., AND WOLFRUM, J. (1969). Reaction of atomic hydrogen with hydrazine. *Ber. Bunsenges. Phys. Chem.* **73**, 956.
- GORDEN, S., MULAC, W., AND NANGIA, P. (1971). Pulse radiolysis of ammonia gas. II. Rate of disappearance of the NH₂(X²B₁) radical. *J. Phys. Chem.* **75**, 2087.
- HAM, D. O., TRAINOR, D. W., AND KAUFMAN, F. (1970). Gas phase kinetics of H + H + H₂ → 2H₂. *J. Chem. Phys.* **53**, 4395.
- HUNTEN, D. M. (1976). Atmospheres and ionospheres. In *Jupiter* (T. Gehrels, Ed.), p. 21. University of Arizona, Tucson.
- LINDZEN, R. S. (1971). In *Mesospheric Models and Related Experiments* (G. Fiocco, Ed.), p. 122. Reidel, Dordrecht.
- SAGAN, C., AND SALPETER, E. E. (1976). Particles, environments, and possible ecologies in the Jovian atmosphere. *Astrophys. J.* **32**, 737.
- SCHÜRIGERS, M., AND WELGE, K. H. (1968). Absorptionkoeffizient von H₂O₂ und N₂H₄ zwischen 1200 und 2000 Å. *Z. Naturforsch. A* **23**, 1508.
- SCHURATH, U., UND SCHINDLER, R. N. (1970). The photolysis of hydrazine at 2060 Å in the presence of ethylene. *J. Phys. Chem.* **74**, 3188.
- SCOTT, D. W., OLIVER, G. D., GROSS, M. E., HUBBARD, W. N., and HUFFMAN, H. M. (1949). Hydrazine: Heat capacity, heats of fusion and vaporization, vapor pressure, entropy and thermodynamic functions. *J. Amer. Chem. Soc.* **71**, 2293.
- STIEF, L. J., AND PAYNE, W. A. (1976). Absolute rate parameter for the reaction of atomic hydrogen with hydrazine. *J. Chem. Phys.* **64**, 4892.
- STROBEL, D. F. (1973). The photochemistry of NH₃ in the Jovian atmosphere. *J. Atmos. Sci.* **30**, 1205.
- THOMPSON, B. A., HARTECK, P., AND REEVES, R. R., JR. (1963). Ultraviolet absorption coefficients of CO₂, CO, O₂, H₂O, N₂O, NH₃, NO, SO₂, and CH₄ between 1850 and 4000 Å. *J. Geophys. Res.* **68**, 6431.
- TOMASKO, M. G. (1974). Ammonia absorption relevant to the albedo of Jupiter. II. Interpretation. *Astrophys. J.* **187**, 641.
- WATANABE, K. (1954). Photoionization and total absorption cross section of gases. I. Ionization potential of several molecules. Cross sections of NH₃ and NO. *J. Chem. Phys.* **22**, 1564.